PHYSICAL REVIEW B VOLUME 51, NUMBER 24 15 JUNE 1995-II

Spin-orbit interaction, triplet lifetime, and fine-structure splitting of excitons in highly porous silicon

K. J. Nash, P. D. J. Calcott, and L. T. Canham
Defence Research Agency (RSRE), St. Andrews Road, Great Malvern, Worcestershire WR14 3PS, United Kingdom

R. J. Needs
Cavendish Laboratory, Madingley Road, Cambridge CB3 0HE, United Kingdom

(Received 22 December 1994)

We present a theoretical treatment of the spin-orbit interaction in luminescent porous silicon. We calculate the radiative lifetime of the triplet exciton, which is determined by the spin-orbit interaction, and compare the results with experiment. We discuss previous work on the optically detected magnetic resonance (ODMR) of porous silicon. We show that the spin-orbit interaction causes a substantial fine-structure broadening of the ODMR. Other workers have argued that the large linewidth of the triplet ODMR cannot be explained within the quantum-confinement theory of porous silicon. Our results demonstrate that this argument is incorrect.

I. INTRODUCTION

In 1990 highly porous silicon, made by anodization of silicon wafers in a hydrofluoric acid solution, was shown to give efficient visible photoluminescence (PL) at room temperature.[1] This PL was attributed to quantum-confined carriers in crystalline silicon nanostructures that are formed by the electrochemical etching process.[1] In the last four years several hundred papers have been written on light-emitting porous silicon, and a great deal of experimental work has been reported. Transmission electron microscopy has demonstrated that the main constituent of freshly prepared highly porous silicon is undulating wires of crystalline silicon with mean diameter ≈ 30 Å.[2] Detailed PL spectroscopy has confirmed that for the main visible PL band (the S band) the luminescent state is a quantum-confined exciton, with a large singlet-triplet splitting, in a crystalline silicon structure.[3–6] These conclusions were based on observations of phonon structure in resonantly excited PL,[3–8] and of the temperature dependence of the PL lifetime.[3,5,9–12]

Many papers have been written on the quantum-mechanical theory of the luminescent states.[13–22] These have addressed the most important aspects of the luminescent states, i.e., their energy, radiative lifetime, and radiative efficiency.[13–22] Other properties that are clearly manifested in PL spectra, the exchange splitting and (in resonantly excited spectra) the phonon-assisted transitions, have also been discussed and explained.[3–6,20] The significance of the spin-orbit interaction to the triplet radiative lifetime has been pointed out.[3,5] However, until now, to our knowledge, a theoretical treatment of the spin-orbit interaction, and a detailed discussion of its experimental consequences, have not been given. The present paper is intended to rectify this omission.

The spin-orbit interaction, though weak, has important consequences. It makes the radiative decay of the (otherwise spin forbidden) triplet exciton weakly allowed. It also induces energy splittings in the triplet state, which are too small to be detected in conventional PL spectroscopy, but are large enough to be observable in magnetic-resonance experiments. We present a theory of these phenomena, based upon a perturbation treatment of the spin-orbit interaction. We then compare this theory with published experimental results, both for the triplet radiative lifetime and for optically detected magnetic resonance (ODMR). The interpretations that have been proposed for ODMR experiments are critically discussed.

The rest of this paper is organized as follows. Section II discusses the spin-orbit interaction in silicon, and obtains the basic form of the interaction that is applied in the rest of the paper. Section III calculates the radiative lifetime of the triplet exciton and compares the results with experiment. Section IV discusses ODMR, and the fine-structure splitting of the triplet exciton that is induced by the spin-orbit interaction. Section V discusses the results of this work, and Sec. VI summarizes our conclusions.

II. THE SPIN-ORBIT INTERACTION IN SILICON

The spin-orbit interaction H^{SO} for an exciton has two terms, one for the valence-band (VB) hole and one of the conduction-band (CB) electron. We consider the VB term first. In bulk Si, H^{SO} couples the degenerate VB states at Γ, leading to a 44-meV splitting.[23] For a VB electron in effective-mass theory, H^{SO} can be written as $\lambda \boldsymbol{l}\cdot\mathbf{s}$,[24] where $\mathbf{s}$ is the spin, $\boldsymbol{l}$ is the operator for unity angular momentum, and $\lambda = \frac{2}{3}\times 44$ meV (the sign of λ is reversed for a VB hole). $\boldsymbol{l}$ is the effective angular momentum that acts in the basis of the three degenerate P-like orbitals of the bulk valence-band maximum (VBM).[25] In a quantum-confined structure of irregular shape, the VB degeneracy is completely lifted (Fig. 1). The three VB states are separated by the difference in their quantum-

0163-1829/95/51(24)/17698(10)/$06.00

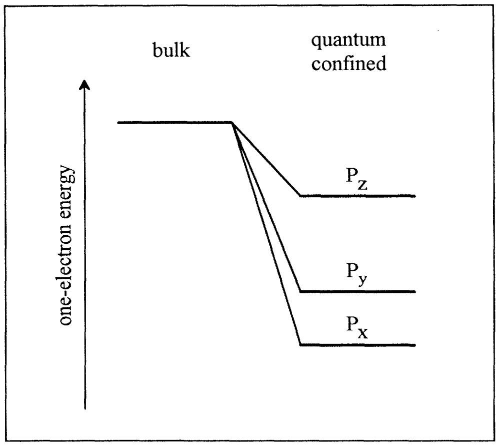

FIG. 1. One-electron energy levels for the highest-energy valence-band states of crystalline silicon, neglecting the spin-orbit interaction. The first column shows the threefold degenerate P orbital for the valence-band maximum of bulk silicon. The second column shows the effect of quantum confinement in an irregular structure. The removal of symmetry lifts the orbital degeneracy of the bulk valence-band maximum. If the coupling between the different P orbitals is ignored, then the quantized energy levels can be labeled in three series, P_x, P_y, and P_z. The highest level of each series is shown in the figure. P_x, P_y, and P_z are orthogonal P orbitals of the effective angular momentum l, where x, y, and z are Cartesian coordinates in a basis determined by the valence-band Hamiltonian for the irregular structure. The energy levels are used in the text as basis states for a perturbation treatment of the spin-orbit interaction.

confinement energies, and are weakly coupled by H^{SO}. The operators l_x, l_y, and l_z are not conserved quantities even in the absence of spin-orbit coupling (in contrast to the bulk $k=0$ no-spin-orbit case), because the Hamiltonian includes the confinement potential for the irregular shape, as well as terms that couple l to the bulk crystal momentum $\mathbf{k}$.[25] The spin-orbit interaction is less important for CB states than for VB states. In bulk Si, H^{SO} couples the conduction-band minimum (CBM) to states with the same crystal momentum, which occur far away in energy (~ 8 eV) from the CBM (the spin-orbit coupling of the CBM to the second CB at ~ 0.5 eV above the CBM vanishes for symmetry reasons). The larger energy denominator makes the electron term in H^{SO} a less important perturbation than the hole term, and so we neglect it. For the same reason, VB to CB matrix elements of H^{SO} can be neglected. In the bulk, the different conduction-band valleys are not coupled by H^{SO} because they occur at different values of crystal momentum. When the translational invariance is removed, e.g., by a donor, a small intervalley spin-orbit interaction (sometimes called the spin-valley interaction) can be detected. For the interstitial Li donor in bulk Si, this spin-valley interaction arises from the spin-orbit interaction of the Si host crystal, and is extremely small, ~ 7 μeV.[26,27] The spin-valley interaction in a Si nanostructure can be compared to the zero-phonon interband radiative transition rate, since both quantities vanish for the bulk and, in quantum-confined systems, are stronger for smaller structures because they depend on the breakdown of momentum conservation. In view of this analogy, matrix elements of the spin-orbit interaction in quantum-confined Si systems are expected, except in structures only a few atoms in size, to be much weaker between states derived from different bulk-Si k values (e.g., the bulk CBM states from different valleys) than for states derived from the same bulk-Si k value (e.g., the bulk VBM states). Therefore we neglect the spin-valley interaction.

A crude calculation of the effects of spin-orbit interaction can be performed as follows: by treating only the hole term of H^{SO}, by assuming that the different quantum-confined VB states are pure P_x, P_y, and P_z states (for a suitable choice of Cartesian axes, not necessarily the cubic crystal axes), with the VBM labeled P_z (Fig. 1), and by including in the calculation only the lowest-energy hole state with each P_i.

We use the basis of (S,m_S) states of the exciton, where S is the total (exciton) spin, and the four basis states are labeled (0,0), (1,1), (1,0), and (1,−1). In this basis,

$$S_z=\begin{bmatrix}0&0&0&0\\0&1&0&0\\0&0&0&0\\0&0&0&-1\end{bmatrix},\quad S^2=\begin{bmatrix}0&0&0&0\\0&2&0&0\\0&0&2&0\\0&0&0&2\end{bmatrix},$$

and the hole spin operators s are

$$s_x=\frac{1}{2\sqrt{2}}\begin{bmatrix}0&1&0&-1\\1&0&1&0\\0&1&0&1\\-1&0&1&0\end{bmatrix},$$

$$s_y=\frac{1}{2\sqrt{2}}\begin{bmatrix}0&i&0&i\\-i&0&-i&0\\0&i&0&-i\\-i&0&i&0\end{bmatrix},$$

$$s_z=\frac{1}{2}\begin{bmatrix}0&0&-1&0\\0&1&0&0\\-1&0&0&0\\0&0&0&-1\end{bmatrix}.$$

From these, the hole term in H^{SO}, $-\lambda \mathbf{l}\cdot\mathbf{s}$, can be constructed.

III. TRIPLET RADIATIVE LIFETIME

The triplet radiative transition rate arises from the coupling by H^{SO} of the triplet exciton to excited-state singlets. The wave function $|\alpha\rangle$ for one of the components of the triplet is perturbed to $|\alpha'\rangle$ by H^{SO}, so that, to first order in H^{SO},

$$|\alpha'\rangle=|\alpha\rangle+\sum_{\nu}{}'\frac{|\nu\rangle H^{\mathrm{SO}}_{\nu\alpha}}{E_\alpha-E_\nu},$$

which leads to a radiative transition rate proportional to

$$I^{\eta}_{\alpha\alpha} = |\langle 0|H^{r\eta}|\alpha'\rangle|^2 = \sum_{\nu,\rho}{}' \frac{H^{r\eta}_{0\nu}H^{\mathrm{SO}}_{\nu\alpha}}{E_\alpha - E_\nu}\,\frac{H^{r\eta}_{\rho 0}H^{\mathrm{SO}}_{\alpha\rho}}{E_\alpha - E_\rho}\,, \tag{1}$$

where $H^{r\eta}$ is the electronic factor of the operator for radiative transitions with polarization η, and the subscript 0 refers to the ground state. With the simplified VB structure mentioned above, the lowest-energy triplet exciton has a P_z VB state, and is coupled by H^{SO} to the singlet excitons ν with P_x and P_y VB states. We assume that the value of $|H^{r\eta}_{0\nu}|^2$ for these states is equal to that for the lowest singlet exciton (with P_z VB state). The $\rho \neq \nu$ terms in Eq. (1) vanish for this simplified VB structure. Adding the transition rates for different polarizations η, one finds

$$\tau^{-1}_{T\alpha\alpha} = \tau_S^{-1} \sum_{\nu}{}^{S} \frac{|H^{\mathrm{SO}}_{\nu\alpha}|^2}{(E_\alpha - E_\nu)^2}\,, \tag{2}$$

where $\sum^S$ represents a sum over singlet states only, τ_S^{-1} is the radiative transition rate for the lowest singlet exciton, and $\tau^{-1}_{T\alpha\alpha}$ is the radiative transition rate for the triplet exciton state α. Summing over the singlet excitons ν with P_x and P_y VB states, and averaging over the three triplet states α, one finds

$$\tau_T^{-1} = \frac{\lambda^2}{6(E_x - E_z)^2}\tau_S^{-1}\,, \tag{3}$$

where the energy denominator is now expressed in terms of the energies E_i ($i = x$, y, and z) for P_i VB hole states, and $E_y = E_x$ is assumed. Equations (2) and (3) remain true if phonon-assisted radiative transitions are included. Each transition rate is an incoherent sum of the zero-phonon rate and the phonon-assisted rate. The latter is summed over the different phonon modes. The phonon-assisted transitions can be represented in Eq. (1) by replacing $H^{r\eta}_{0\nu}$ with the electronic factor of the second-order matrix element[28] for phonon-assisted radiative transitions with polarization η.

To compute τ_T^{-1} we must first determine the VB energy splitting $E_x - E_z$. This quantity is poorly known, as will become clear in the final paragraph of this section, and so instead we compare our theory with the experimental variation of τ_T/τ_S as a function of band-gap upshift energy E_{up}. We also obtain a value of $(E_x - E_z)$ from the experimental results, for use in Sec. IV C.

We begin by analyzing experimental values of τ_T/τ_S, the ratio of triplet and singlet radiative lifetimes. τ_T/τ_S is obtained from measurements of the PL lifetime as a function of temperature,[3,5] with a constant correction factor to allow for nonradiative processes (this correction is discussed in the next paragraph). τ_T/τ_S is plotted in Fig. 2 as a function of band-gap upshift energy E_{up}, which is estimated as $E_{\mathrm{PL}} - 1.0$ eV (i.e., as the PL energy, less the bulk-Si band-gap energy of 1.1 eV, plus 0.1 eV for E_B, the estimated sum of exciton localization and binding energies[13]). In effective-mass theory (EMT), $E_x - E_z$ is proportional to E_{up} in structures with the same shape but different sizes. Thus Eq. (3), together with EMT, predicts $\tau_T/\tau_S \propto E^2_{\mathrm{up}}$. The experimental points are a good fit to $\tau_T/\tau_S \propto E^n_{\mathrm{up}}$, with best-fit exponent $n = 2.49 \pm 0.07$ (Fig. 2). The best-fit exponent for the points with $E_{\mathrm{PL}} < 1.75$ eV is 2.01 ± 0.12 (Fig. 2); as expected, the EMT result is a better approximation for smaller values of E_{up}. The errors quoted represent the standard deviation of the fitting parameter. As is found for the exchange splitting,[3] EMT gives good qualitative agreement with experiment, but does not give exact quantitative agreement. This reflects the inaccuracy of EMT itself, particularly at larger values of E_{up}. The assumption that E_B is independent of E_{PL} also loses accuracy at larger values of E_{up}. It is notable that the theory correctly predicts the increasing trend of τ_S/τ_S with E_{up}, i.e., that the decrease of τ_T with E_{up} is not as rapid as the decrease of τ_S.[3]

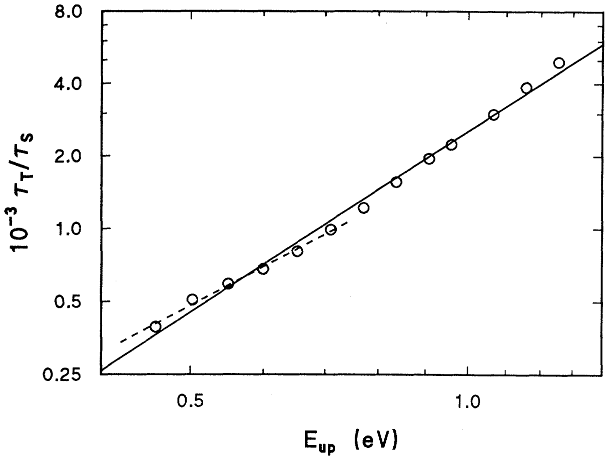

FIG. 2. The ratio of triplet and singlet radiative lifetimes, τ_T/τ_S, plotted against the estimated band-gap upshift E_{up} on logarithmic scales. E_{up} is estimated as $E_{\mathrm{PL}} - 1.0$ eV (see text). The points are experimental values of τ_T/τ_S, obtained from Refs. 3 and 5 and corrected for the nonradiative contribution by multiplying by three (see text). The solid line is the best straight-line fit to all the points, and gives an exponent of 2.49. The dashed line is the best straight-line fit to the points with $E_{\mathrm{up}} < 0.75$ eV, and gives an exponent of 2.01.

To obtain a value of $E_x - E_z$ for use in Sec. IV C, we use the experimental results for $E_{\mathrm{PL}} = 1.71$ eV:[3,5] $\tau_T = 4.89$ ms and $\tau_S = 14.8$ μs. The experimental PL lifetimes include a nonradiative contribution, whereas Eq. (3) requires the radiative lifetime. A threefold decrease in PL intensity is found when the temperature is reduced to the low values at which τ_T is determined.[5] This is most reasonably interpreted as a lower radiative efficiency for the long-lived triplet state[5] (an alternative interpretation is discussed in Sec. V). The ratio τ_T/τ_S is therefore multiplied by 3 to allow for this change in efficiency. Thus $\tau_T^{-1}/\tau_S^{-1} \approx 1.0 \times 10^{-3}$, from which Eq. (3) gives $(E_x - E_z) = 0.38$ eV.

This value of $(E_x - E_z)$, estimated from the experimental singlet and triplet lifetimes, can be checked against theoretical expectations (an independent experimental measure is not available). It is convenient to express the

VB splitting $(E_x - E_z)$ in terms of the downshift E_z of the VBM, by defining the ratio $R = (E_x - E_z)/E_z$. The band-gap upshift is estimated as 0.71 eV. From the photoemission and x-ray-absorption spectroscopy of Ref. 29, we estimate that the downshift E_z of the VBM is $\sim\frac{2}{3}$ of this, i.e., 0.47 eV. Thus we estimate R to be 0.80. We require a value of R from electronic-structure calculations, for comparison with this result. However, the value of R is strongly dependent on geometry. First-principles calculations[13-22] have been performed only on special structures which, for the purpose of estimating R, are not representative of porous silicon (the reason for this will be discussed shortly). Therefore the theoretical value of R is unclear, and we can only consider the range of possible values. In bulk Si the ratio R in EMT varies from $6\gamma_2/(\gamma_1 - 2\gamma_2) = 0.56$ in the $\langle 001 \rangle$ directions to $6\gamma_3/(\gamma_1 - 2\gamma_3) = 6.23$ in the $\langle 111 \rangle$ directions, where γ_n ($n = 1$, 2, and 3) are the Luttinger parameters.[30] For a wire with [001] orientation and (110) and $(1\bar{1}0)$ surfaces, the approximate EMT result $3\gamma_2/(\gamma_1 - 2\gamma_2) = 0.28$ is obtained;[22] in a first-principles calculation for a 9×8 wire, a mean value of 0.20 is found, but the lowest state is not the same as in EMT.[22] For structures other than this special type of wire, the EMT value of R will involve the large γ_3 as well as the much smaller γ_2. The larger value of R means that, in a first-principles calculation for a general structure, R is expected to be larger than for the [001] wire with (110) and $(1\bar{1}0)$ surfaces, and the level ordering is likely to be the same as in EMT. The values of R discussed above bracket the result $R = 0.80$ obtained from experimental results by our estimates of $(E_x - E_z) = 0.38$ eV and $E_z = 0.71 \text{ eV} \times \frac{2}{3} = 0.47$ eV. We conclude that the estimate of $(E_x - E_z)$ is consistent with our limited knowledge of quantum-confined energy levels in irregular crystalline silicon structures.

IV. FINE STRUCTURE OF THE TRIPLET

A. Optically detected magnetic resonance (ODMR) and the triplet exciton

The triplet exciton state has very small energy splittings, of the order of 1 μeV to a few tens of μeV [Fig. 3(a)]. This fine structure can be expressed as a term in the spin Hamiltonian, and, if it is not too large, can be probed by optically detected magnetic resonance (ODMR).[32,33] The spin Hamiltonian H for a triplet is the secular matrix for this threefold-degenerate state, expressed in terms of effective spin operators for spin unity.[34-36] The interactions with other states of the system are treated by perturbation theory and included in H. In general, the spin Hamiltonian gives a complete description of the small number of energy levels between which magnetic-resonance transitions occur, and is the most convenient interface between theory and experiment.[35] Section IV B examines the spin Hamiltonian for the triplet exciton in porous silicon, and the general properties of the consequent ODMR.

The information available from ODMR experiments must be interpreted with care. The attribution of ODMR signals is always difficult, because ODMR signals can arise from magnetic resonance not only in the initial state of PL, but alternatively in a feeder state or in a shunt state (see, for example, Ref. 33). Also, when two spectrally broad PL bands coincide in wavelength, one band may dominate the overall PL intensity while the other dominates the ODMR signal.[37] Furthermore, although ideally the complete spin Hamiltonian can be deduced from ODMR experiments, it does not always convey direct information about the *chemical* identity of the host material, particularly when there is no resolved hyperfine structure. The lack of chemical information is evident in the spin Hamiltonian of Eq. (4) and the subsequent discussion in Sec. IV B. In particular, the assertion that the similarity of the ODMR spectra for different materials (porous silicon and siloxene) "provides conclusive evidence for the existence of a common radiative center" (Ref. 38) is unjustified.

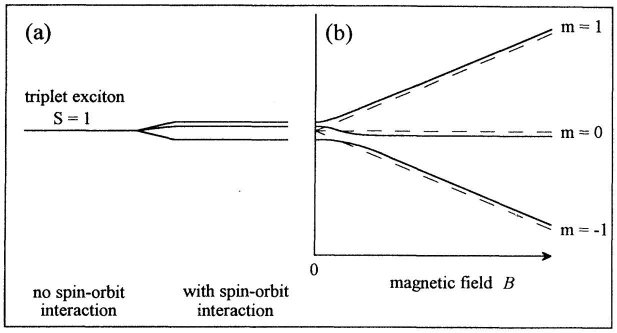

FIG. 3. The extremely small splittings of the lowest-energy triplet exciton. (a) The first column shows the triplet exciton. The only degeneracy is the threefold spin degeneracy. The second column shows the splitting of this triplet state by the second-order spin-orbit interaction. The threefold degeneracy is lifted. (b) The effect of magnetic field B. The solid lines represent the energy levels. The dashed lines are the energy levels in the absence of second-order spin-orbit splittings. At $B = 0$ the states are those shown in the second column of (a). At high B, the second-order spin-orbit interaction is a small perturbation compared to the magnetic field. In the high-B limit, the $m = 1$ and -1 states are shifted equally by this perturbation, so that the $\Delta m = 2$ transition energy is unchanged by the second-order spin-orbit interaction. The shift of the $m = 0$ state is different, so that the $\Delta m = \pm 1$ transition energies are altered by the second-order spin-orbit interaction.

There are several reports of ODMR experiments on porous silicon. The first was by Lane *et al.*,[39] who observed sharp PL-enhancing resonances [with a full width at half maximum (FWHM) < 25 G] at $g \approx 2$. Subsequent ODMR experiments have been reported by Stutzmann and co-workers,[40-47] by Meyer and co-workers,[48-50] and by Mochizuki and Mizuta.[51] References 40–47 observe a broad (FWHM ≈ 500 G) enhancing resonance with a Gaussian line shape, together with a weaker but sharper (FWHM ≈ 150 G) resonance at half the magnetic field, which they attribute to the $\Delta m = \pm 1$ $(g = 2)$ and ± 2 $(g = 4)$ resonances, respectively, of the triplet initial state of PL. They also observe a sharp (FWHM < 25 G) quenching resonance at $g \approx 2$ which they attribute to the

P_b center. The P_b center was identified in electron-spin resonance (ESR) of the same samples.[40] The characteristic anisotropy of the P_b resonance was observed directly in ODMR of porous silicon by Ref. 48. References 48–50 concentrate on the spectral dependence of the P_b ODMR signal, and on other ODMR signals of the ~1 eV PL band, but do not discuss other ODMR signals of the S-band PL (i.e., the band due to quantum-confined excitons, which peaks at ~1.5 eV in the samples of Ref. 48). Reference 51 discusses mainly the ~1-eV PL band (this band will not be considered further in the present work), and detects no ODMR signal on the S-band PL, possibly due to a lack of sensitivity. Reference 48 points out that the sign of the P_b ODMR signal (quenching or enhancing) for the S band is different in different studies[40,47] and can be reversed by thermal oxidation. The P_b resonance takes place in a single-electron ($S=\frac{1}{2}$) state with an anisotropic g factor, and, for the S band, is an example of an ODMR signal that is believed to take place in a shunt state or feeder state rather than in the initial state of PL. In all these ODMR studies,[39,40,48,51] additional sharp-line $g \approx 2$ resonances were found, whose origin is not properly understood.

B. The spin Hamiltonian for the luminescent triplet

The spin Hamiltonian for the lowest exciton triplet is

$$H=\sum_{i,j} D_{ij} S_i S_j + \mu_B \sum_{i,j} g_{ij} B_i S_j \; , \tag{4}$$

where subscripts i,j refer to Cartesian components, $\mathbf{B}$ is the magnetic field, μ_B is the Bohr magneton, g_{ij} is the g tensor, S_i's are the spin operators for spin unity, and D_{ij} is the fine-structure tensor. The first term in Eq. (4) is the zero-field-splitting or fine-structure term. The second term is the linear Zeeman term. The hyperfine interaction of the exciton spin with the nuclear spins (of ^{29}Si and ^{1}H) is negligible because the exciton extends over many atomic sites. Equation (4) is the most general spin Hamiltonian that includes a zero-field splitting and a linear Zeeman effect, for the $S=1$ case. The energy levels for this spin Hamiltonian as a function of magnetic field are shown in Fig. 3(b).

For the resonance lines so far reported in porous Si, and in many other cases where spin-orbit interactions are weak, g_{ij} is close to $2\delta_{ij}$. D_{ij} is real and symmetric, and so can be diagonalized. When expressed in terms of the principal axes X, Y, and Z of D_{ij}, the first term of Eq. (4) is

$$C+D\{S_Z^2-\tfrac{1}{3}S(S+1)\}+E(S_X^2-S_Y^2) \tag{5}$$

and the energy levels, ignoring the constant C, are $-\frac{2}{3}D$ (Z-like state), $\frac{1}{3}D+E$ (Y-like state), and $\frac{1}{3}D-E$ (X-like state).

For large B, the D_{ij} term can be treated as a small perturbation. This is the usual regime in magnetic resonance. The unperturbed spin states are the $m=1$, 0, and -1 states of the spin component $\hat{\mathbf{n}}\cdot\mathbf{S}$, where $n_j=\sum g_{ij}B_i$, and the caret (^) indicates normalization. The first-order shift is the same for the $m=1$ and -1 levels, but different for the $m=0$ level. This means that, at least in first-order perturbation theory, the energy of the $m=-1$ to $m=1$ transition ($\Delta m=2$ transition) is unperturbed by D_{ij} and is therefore sharp. The energies of the $m=0$ to $m=\pm 1$ transitions ($\Delta m=\pm 1$ transitions), in contrast, are perturbed by D_{ij}. In porous silicon the excitons are confined by structures with a variety of shapes, sizes, and orientations with respect to $\mathbf{B}$, so that different triplet excitons will have different $\Delta m=\pm 1$ transition energies, leading to a broad overall feature for the $\Delta m=\pm 1$ transitions. The random orientation of the principal axes of D_{ij} with respect to $\mathbf{B}$ leads to a so-called powder pattern in the ODMR spectrum.[52] This broad spectrum exhibits structure related to the values of D and E. However, the addition of random terms to D and E, resulting from the variety of sizes and shapes of confining structures, leads to a broader, structureless ODMR spectrum.[52] This is an example of how a magnetic-resonance transition can be inhomogeneously broadened when the resonant state has a variety of environments. The broad $\Delta m=\pm 1$ line and comparatively sharp $\Delta m=\pm 2$ line predicted by theory are consistent with the ODMR signals that Refs. 40–47 assign to a triplet (see Sec. IV A above).

The width of the ODMR line can be expressed in terms of the parameters D and E of Eq. (5). If for simplicity we neglect the E term, then the fine-structure splitting at zero field is equal to D. Performing the perturbation theory mentioned in the previous paragraph for the large-B case, the fine-structure shift E_{fs} of the $m=0$ level less that for $m=\pm 1$ is $E_{\mathrm{fs}}=(\frac{1}{3}-\hat{n}_Z^2)\frac{3}{2}D$. If all orientations of the principal axes of D_{ij} relative to $\mathbf{B}$ are considered, then the mean value of E_{fs} is zero, and the root-mean-square (rms) value σ_{fs} of E_{fs} is

$$\sigma_{\mathrm{fs}}=D/\sqrt{5} \; . \tag{6}$$

C. Dipole-dipole interaction and second-order spin-orbit interaction

The fine-structure tensor D_{ij} arises from two distinct physical mechanisms: the magnetic dipole-dipole interaction of the electron and hole, and the second-order spin-orbit interaction. Here we investigate the second-order spin-orbit interaction. The much weaker dipole-dipole interaction is discussed in Sec. V. The spin-orbit interaction also gives rise to a small correction to the g_{ij} tensor (see the Appendix).

Treating the spin-orbit interaction H^{SO} to second order, its contribution to the spin Hamiltonian is

$$H_{\alpha\beta}=\sum_{\nu}\frac{H^{\mathrm{SO}}_{\alpha\nu}H^{\mathrm{SO}}_{\nu\beta}}{E_\alpha-E_\nu} \; , \tag{7}$$

where the states α and β belong to the lowest-energy triplet, and the excited states ν do not. $H^{\mathrm{SO}}=-\lambda \boldsymbol{l}\cdot\mathbf{s}$ (Sec. II). The operators l_i couple the P_z hole ground state to the P_x and P_y excited states. H^{SO} couples the lowest exciton state, with P_z VB wave function, to excited states of the exciton [labeled ν in Eq. (7)] with P_x and P_y VB wave functions. If the exchange splitting of the exciton excited states ν is ignored, then Eq. (7) reduces to

$$H_{\alpha\beta} = A\delta_{\alpha\beta} \ , \tag{8}$$

where A is a constant, i.e., the second-order spin-orbit interaction causes only a uniform shift of the three states of the lowest triplet,[53] which cannot be detected by magnetic resonance. However, if the exchange splitting of the excited states ν is taken into account, then a zero-field-splitting term arises in the spin Hamiltonian:

$$H_{\alpha\beta} = \sum_{\nu}{}^{T} \frac{H^{\mathrm{SO}}_{\alpha\nu} H^{\mathrm{SO}}_{\nu\beta}}{E_\alpha - E^T_\nu} + \sum_{\nu}{}^{S} \frac{H^{\mathrm{SO}}_{\alpha\nu} H^{\mathrm{SO}}_{\nu\beta}}{E_\alpha - E^T_\nu - \Delta_\nu} \ ,$$

where $\sum^T$ and $\sum^S$ denote sums over triplet states and singlet states, respectively, and Δ_ν is the exchange splitting of ν, i.e., the energy difference of the singlet and triplet forms of ν. E^T_ν is the energy of the triplet form of ν (equal to E_ν if ν is a triplet and $E_\nu - \Delta_\nu$ if ν is a singlet). Thus, performing a binomial expansion of the denominator of the second sum,

$$\begin{aligned} H_{\alpha\beta} &= \sum_{\nu} \frac{H^{\mathrm{SO}}_{\alpha\nu} H^{\mathrm{SO}}_{\nu\beta}}{E_\alpha - E^T_\nu} + \sum_{\nu}{}^{S} \frac{H^{\mathrm{SO}}_{\alpha\nu} H^{\mathrm{SO}}_{\nu\beta} \Delta_\nu}{(E_\alpha - E^T_\nu)^2} \\ &= A\delta_{\alpha\beta} + \sum_{\nu}{}^{S} \frac{H^{\mathrm{SO}}_{\alpha\nu} H^{\mathrm{SO}}_{\nu\beta} \Delta_\nu}{(E_\alpha - E^T_\nu)^2} \\ &= A\delta_{\alpha\beta} + \frac{\Delta_x \lambda^2}{8(E_x - E_z)^2} \begin{bmatrix} 1 & 0 & 1 \\ 0 & 0 & 0 \\ 1 & 0 & 1 \end{bmatrix} \\ &\quad + \frac{\Delta_y \lambda^2}{8(E_y - E_z)^2} \begin{bmatrix} 1 & 0 & -1 \\ 0 & 0 & 0 \\ -1 & 0 & 1 \end{bmatrix} . \end{aligned}$$

In the second step, the $\Delta_\nu = 0$ result (8) is used, and the zero-field splitting is expressed as a sum over singlet states only, like the triplet radiative lifetime [Eq. (2)]. In the last step, the sum is performed over singlet exciton states ν with P_x and P_y VB states. The 3×3 matrices are expressed in the basis of $m_s = 1$, 0, and -1 triplet states. In terms of the constants defined in Eq. (5), the result is

$$D = \frac{\lambda^2}{8} \left[\frac{\Delta_x}{(E_x - E_z)^2} + \frac{\Delta_y}{(E_y - E_z)^2} \right] \ ,$$

$$E = \frac{\lambda^2}{8} \left[\frac{\Delta_x}{(E_x - E_z)^2} - \frac{\Delta_y}{(E_y - E_z)^2} \right] .$$

(Also, the principal axes X, Y, and Z of D_{ij} [Eq. (5)] coincide with the Cartesian axes x, y, and z defined in Sec. II; this result is a consequence of our simple model of the quantum-confined VB states, which is implicit in the definition of x, y, and z.)

Assuming that $\Delta_y = \Delta_x$ and $E_y = E_x$, and using the value of $(E_x - E_z)$ found in Sec. III for $E_{\mathrm{PL}} = 1.71$ eV, one finds

$$D = 18\ \mu\mathrm{eV} \frac{\Delta_x}{\Delta} \tag{9}$$

where $\Delta = 12.1$ meV is the exchange splitting of the lowest-energy exciton states. This calculated value of D will be interpreted and discussed in Sec. V. For comparison with the experimental linewidths given in Sec. IV A, the relation between a fine-structure energy shift $\delta\varepsilon$ and the resulting magnetic field shift δB in fixed-frequency ODMR is required. This can be deduced, from Eq. (4) and the relation $g_{ij} \approx 2\delta_{ij}$, as

$$\delta\varepsilon \approx 2\mu_B \delta B \ .$$

Thus an energy of 18 μeV corresponds to a magnetic field of 1600 G.

A brief account of the electron-hole exchange interaction in silicon will assist the subsequent discussion. Combining the results of Ref. 54 for indirect-gap semiconductors with the EMT results of Ref. 55 for bound excitons, the exchange splitting for a discrete exciton in which the electron occupies only one of the conduction-band valleys in k space is

$$\Delta = \sum_{i,j} J_{ij} \int d^3\mathbf{r}\, \varphi_i^*(\mathbf{r},\mathbf{r}) \varphi_j(\mathbf{r},\mathbf{r}) \ ,$$

where

$$\varphi_i(\mathbf{r}_e,\mathbf{r}_h) \equiv [\varphi_x(\mathbf{r}_e,\mathbf{r}_h), \varphi_y(\mathbf{r}_e,\mathbf{r}_h), \varphi_z(\mathbf{r}_e,\mathbf{r}_h)] \tag{10}$$

is the envelope function for the exciton. The three components ($i = x$, y, and z) multiply the three P_i-like band-edge Bloch functions of the bulk-Si valence band at Γ. J_{ij} is a second-rank tensor which, when expressed in terms of the cubic crystal axes (not the axes used elsewhere in this paper), for the case in which the electron occupies the [001] conduction-band valley, has the form

$$J_{ij} = J_I \begin{bmatrix} 1 & 0 & 0 \\ 0 & 1 & 0 \\ 0 & 0 & 1 \end{bmatrix} + J_A \begin{bmatrix} 0 & 0 & 0 \\ 0 & 0 & 0 \\ 0 & 0 & 1 \end{bmatrix} .$$

J_I and J_A are the coefficients of isotropic and anisotropic terms in J_{ij}, respectively.

Because the second-order spin-orbit term in D_{ij} turns out, through cancellations between terms from singlet and triplet excited states, to be proportional to $\lambda^2\Delta/(E_x - E_z)^2$ rather than to $\lambda^2/(E_x - E_z)$, it is necessary to check for other terms that are of order $\lambda^2\Delta/(E_x - E_z)^2$, in case there are further cancellations. Such terms are of two types: the first type comprises terms similar to those calculated above, but which involve off-diagonal matrix elements of the exchange interaction (in the present simple theory, these matrix elements exist only for the J_A term of the exchange interaction, and couple the excitons with different VB states P_i); the second type comprises terms that are second order both in the spin-orbit interaction and in the off-diagonal part of the exchange interaction, but which involve as an intermediate state the lowest singlet state of the exciton, with energy denominator Δ rather than $(E_x - E_z)$: therefore these terms are of order $\lambda^2\Delta/(E_x - E_z)^2$ overall. Both types of terms depend on the orientation of the VB principal axes defined in Sec. II with respect to the cubic crystal axes, and so differ from one triplet exciton to another. Neither term alters the basic energy scale of D_{ij} computed above, and both contribute to inhomogeneous broadening of the ODMR. These are the only terms

$\lambda^m\Delta^n/(E_x-E_z)^{m+n-1}$ with $m=2$ and $n=1$. No other terms $\lambda^m\Delta^n/(E_x-E_z)^{m+n-1}$ with $m+n\leq 3$ contribute to the fine-structure splitting.

Even with the corrections discussed in the preceding paragraph, the calculation of D_{ij} given above is crude because it simplifies the valence-band structure by ignoring both the $P_x/P_y/P_z$ mixing and the excited states in each P_i series; it uses a crude estimate of the VB energy splitting E_x-E_z, it neglects the electron term in H^{SO}, and it neglects the breakdown of EMT that occurs in small structures, most obviously the breakdown of the EMT formula $\lambda \mathbf{l}\cdot\mathbf{s}$ (Ref. 24) for the hole spin-orbit coupling. The calculation is not intended as a complete theory of triplet ODMR in porous silicon.

V. DISCUSSION

Because the low-T luminescent state for the S band in porous silicon is believed to be a triplet exciton,[3-6] and because triplet luminescent states often exhibit strong ODMR, it is tempting to suggest that some of the ODMR signals found in experiments can be attributed to the triplet initial state of PL. One property expected for the ODMR signal of the triplet initial state of PL is that it will occur only at low temperature:[3] as the temperature is raised, the singlet PL (with no initial-state ODMR signal) quickly dominates over the triplet PL. Although the majority of excitons still occupy the triplet state, the triplet PL is overwhelmed by the singlet PL because the latter has a much higher radiative transition rate. The ODMR reported in Ref. 39 has this temperature dependence, and the consistency of this property with expectations for a singlet/triplet exciton was pointed out in Ref. 3. However, given the large linewidth estimated by theory (Sec. IV C), this resonance appears to be too narrow (<25 G) to be consistent with attribution to the triplet initial state of PL. A rapid decrease of ODMR signal with increasing T was also reported for the broad ODMR found in siloxene,[45] but the T dependence of the porous silicon ODMR was not discussed in Refs. 40–47. The ODMR experiments of Refs. 48–50 were limited to very low temperatures.

Given the large linewidth expected for the ODMR of the triplet initial state of PL (Sec. IV C), the broad signal found in Refs. 40–47 is a promising candidate for the initial-state resonance. Evidence for the triplet origin of this signal is provided by the observation of $\Delta m=\pm 2$ transitions,[40-47] and by the fact that the latter are sharper than the main $\Delta m=\pm 1$ line (Sec. IV B). The experimental FWHM of the $\Delta m=\pm 1$ transition is 500 G (5.8 μeV), which for this Gaussian line shape implies a standard deviation of $\sigma_{\mathrm{fs}}=213$ G (2.5 μeV). If the whole of this linewidth is attributed to the random orientation of the principal axes of D_{ij}, then Eq. (6) gives $D=480$ G (5.5 μeV). If $\Delta_x=\Delta$ in Eq. (9), then the theoretical value of D is ~ 3 times larger than this experimental value. Given the approximations made in the calculation of D and noted at the end of Sec. IV C, the agreement with the value of D deduced from the 500-G-wide resonance is satisfactory. The calculated D might be reduced not only by improving these approximations, but also if Δ_x is smaller than Δ. This might possibly occur if excitons formed from P_x and P_y valence-band states are less strongly localized than the low-energy exciton formed from the VBM P_z state. Alternatively, the linear combination of J_I and J_A that is appropriate for P_x and P_y excitons might be smaller than for P_z excitons. Another possibility that cannot yet be ruled out is that the ODMR of the initial state of PL has not yet been detected, and that the 500-G-wide resonance of Refs. 40–47 arises in a triplet state other than the initial state of PL (see Sec. IV A).

The most important point to note about the results of Sec. IV C is that the contribution of the second-order spin-orbit interaction to the fine-structure splitting of the initial-state triplet is not negligible compared to the measured value of this splitting. As noted in Sec. IV C, the fine-structure tensor D_{ij} has contributions from the second-order spin-orbit interaction and from the magnetic dipole-dipole interaction. Only if the second-order spin-orbit interaction can be neglected can D_{ij} be attributed solely to the dipole-dipole interaction; then the size of D_{ij} can be used to measure the spatial separation L of the electron and hole, with a large D_{ij} indicating small L.[34] This method was used in Refs. 40–47, which assign the broad triplet resonance to the initial state of PL, and attribute the large width to the magnetic dipole-dipole interaction of the electron and hole. From this they deduce that L is small, ≈ 4 Å. References 40–47 conclude that this is consistent with the localization of the exciton in a Si_6 ring in a siloxene-based compound, rather than in the larger (~ 30 Å) crystalline silicon structures of the quantum-confinement model, for which the dipole-dipole D_{ij} (proportional to L^{-3}) is very much smaller. The arguments of Refs. 40–47 are incorrect because, as demonstrated in Sec. IV C, the second-order spin-orbit interaction cannot be neglected. The conclusions of Refs. 40–47—that the length scale of the exciton is very short (≈ 4 Å), and that the large fine-structure splitting cannot be explained in terms of quantum confinement in much larger (~ 30 Å) structures of crystalline silicon—are for this reason invalid. References 40–47 also deduce a short exciton length scale from their ODMR results for siloxene. This conclusion should be treated with caution, until the second-order spin-orbit interaction in siloxene has been properly investigated.

It has been reported that the linewidth of the broad ODMR signal is independent of the PL wavelength,[46,47] and that this result is inconsistent with the quantum-confinement theory. It would be desirable to confirm the experimental result with ODMR measurements of monochromated PL, since the wavelength selection in Refs. 46 and 47 is performed only with low-pass filters: this method is particularly unsatisfactory for resolving the high-energy tail of the PL. Also, it would be helpful to know with more certainty whether the broad resonance can be attributed to the initial state of PL. Nevertheless, it is possible to investigate the predictions of the quantum-confinement model. The arguments of Refs. 46 and 47 on the wavelength dependence of the ODMR linewidth again neglect the second-order spin-orbit interaction, which is the major source of the ODMR linewidth in the quantum-confinement theory. The crude theory of Sec. IV C, together with the experimental results for τ_T, τ_S, and Δ,[3,5] predict a decrease of D from 28 $\mu\text{eV}\times\Delta_x/\Delta$ at $E_{\text{PL}}=1.459$ eV to 9 $\mu\text{eV}\times\Delta_x/\Delta$ at $E_{\text{PL}}=2.254$ eV. However, we emphasize once again that the theory of Sec. IV C makes a number of approximations, and that quantitative knowledge about the excited-state exchange splittings Δ_x and Δ_y as functions of E_{PL} is lacking. Also, the calculation of the dependence on E_{PL} ignores the possibility of a systematic change in shape of the confining structures in a given sample, as a function of E_{PL}.[19] We regard the calculation of Sec. IV C as giving no more than a useful indication of the order of magnitude of the ODMR linewidth.

Finally, it should be noted that the experimental study of the broad triplet ODMR signal is still at an early stage. In contrast to the phonon structure in resonantly excited PL,[3–8] and the temperature dependence of the PL lifetime,[3,5,9–12] which provides evidence of the singlet-triplet splitting of the luminescent exciton, the broad triplet ODMR has so far been observed in only one laboratory.[40–47] Furthermore, the intensity of this ODMR signal is perhaps rather low for a triplet initial state whose luminescence is believed to compete with faster nonradiative recombination. These nonradiative processes were invoked to explain the decrease in PL intensity at low temperatures (Sec. III). If, instead, the radiative efficiency of the luminescent states is assumed to be constant, and the decrease in PL intensity is attributed to a temperature dependence of the feeder processes that create luminescent or nonluminescent states, then the measured value of τ_T^{-1}/τ_S^{-1} does not require the correction factor applied in Sec. III. With this assumption, $\tau_T^{-1}/\tau_S^{-1}\approx 3\times 10^{-3}$ at $E_{\text{PL}}=1.71$ eV, and the calculation in the last two paragraphs of Sec. III would produce the results $E_x-E_z=0.22$ eV and $R=0.46$. These values lead to $D=54\ \mu\text{eV}\times\Delta_x/\Delta$ in place of Eq. (9). If the PL efficiency is high, then the ODMR signal will be weak. In this case, the initial-state resonance would be more readily detected as a change in PL lifetime, by using time-resolved ODMR. If there really are resonances as broad as 54 μeV (4700 G), these would be more conveniently observed at higher microwave frequencies than at the X-band ($\sim$9 GHz) frequencies used in Refs. 39–47.

VI. CONCLUSIONS

In summary, we have investigated the effect of spin-orbit interaction on the exciton states of highly porous silicon. The spin-orbit interaction is a weak perturbation, but it has an important effect on the triplet exciton. First, the triplet radiative lifetime, which is infinite if spin-orbit coupling is neglected, acquires a finite value. The measured lifetime, and its dependence on PL energy, are consistent with the theory. Second, the degeneracy of the triplet state is lifted, implying an inhomogeneous fine-structure broadening of ODMR. Stutzmann and coworkers observed a triplet resonance in ODMR, which they attribute to the excitonic initial state of PL. Their analysis of the large ODMR linewidth appeared to indicate much more strongly confined excitons than could be explained by quantum confinement. However, their analysis overlooked the spin-orbit interaction. Instead, it attributed the fine-structure broadening to the much weaker magnetic dipole-dipole interaction of the electron and hole; within this model, the large ODMR linewidth implies that the exciton is much more localized ($\approx$4 Å) than in the quantum-confinement theory ($\approx$30 Å). Our simple calculation shows that the large broadening can be explained within the quantum-confinement model, if the spin-orbit interaction is included. The argument[40–47] that the large ODMR linewidth implies an exciton so compact as to be incompatible with the quantum-confinement theory is therefore invalid.

ACKNOWLEDGMENTS

The authors are grateful to T. I. Cox and M. J. Kane for a critical reading of the manuscript.

APPENDIX: MODIFICATION OF THE *g* FACTOR

The g_{ij} tensor of the spin Hamiltonian is altered by the spin-orbit interaction. The basis states used in the perturbation theory of the present work are calculated with neither the spin-orbit interaction H^{SO} nor the Zeeman interaction H^Z. A perturbation treatment of H^Z+H^{SO} gives rise to terms in the spin Hamiltonian (Sec. IV B). The basic g factor $g_{ij}=2\delta_{ij}$ arises in first order; the correction to g_{ij} arises in second order. There are three terms in the second-order treatment of H^Z+H^{SO}. The term in $(H^{\text{SO}})^2$ is the second-order spin-orbit interaction discussed in Sec. IV C. The term in $(H^Z)^2$ contributes to the spin Hamiltonian a very small term that is quadratic in magnetic field. g_{ij} is modified by the term in the spin Hamiltonian of order $H^Z\times H^{\text{SO}}$; this term is [cf. Eq. (7)]

$$H_{\alpha\beta}=\sum_{\nu}\frac{H^{\text{SO}}_{\alpha\nu}H^{Z}_{\nu\beta}+H^{Z}_{\alpha\nu}H^{\text{SO}}_{\nu\beta}}{E_\alpha-E_\nu}\ , \tag{A1}$$

where α, β, and ν are defined as in Eq. (7); H^Z is given by Ref. 25 as

$$H^Z=\mu_B\mathbf{B}\cdot(Km\mathbf{l}+g_e\mathbf{s}_e+g_h\mathbf{s})+H^{ze}\ ;$$

m is the free-electron mass; $\mathbf{s}_e$ is the electron spin; and H^{ze} is the term from the Luttinger EMT Hamiltonian that involves the vector potential $\mathbf{A}$ and the envelope-function momenta $\mathbf{p}_e$ and $\mathbf{p}_h$. g_e, the electron g factor, and g_h, the spin-only hole g factor, are close to 2, so that $g_e\mathbf{s}_e+g_h\mathbf{s}=2\mathbf{S}$. Cyclotron resonance gives the experimental value for the Luttinger parameter κ,[25] from which Km can be determined using the relation $Km=-(1+3\kappa)$.[25] Small corrections to this relation, and to the value of g_h, arise from a generalization of Luttinger's approach to include an arbitrarily strong (rather than an infinitely weak) spin-orbit interaction.[56] These corrections are negligible for silicon because the spin-orbit interaction is weak. The experimental value $\kappa=-0.42$ thus implies $Km=0.26$.[30]

In the simple theory of the present work, the VB states are pure P_x, P_y, or P_z states of the operator $\boldsymbol{l}$. Thus H^{SO} couples the P_z ground state to P_x and P_y states but not to P_z states. The three terms in H^z behave differently in Eq. (A1), depending on whether they couple P_x and P_y states back to P_z states.

(1) The $\mathbf{B}\cdot(g_e\mathbf{s}_e+g_h\mathbf{s})$ term in H^z does not alter the P_i state or the envelope function, and so does not contribute to the $H^z\times H^{\mathrm{SO}}$ term of $H_{\alpha\beta}$ [Eq. (A1)].

(2) The $\mathbf{B}\cdot\boldsymbol{l}$ term couples the P_x and P_y excited states back to the P_z ground state: its contribution to $H_{\alpha\beta}$ corresponds to a change in g_{ij} of

$$\frac{\lambda K m}{E_x-E_z}\delta_{iy}\delta_{jy}+\frac{\lambda K m}{E_y-E_z}\delta_{ix}\delta_{jx} .$$

If we set $E_x-E_z=E_y-E_z=0.38$ eV, as in Sec. IV C, then g is increased by $\delta g=0.02$ for magnetic field $\mathbf{B}$ along the x or y directions, but is unchanged for $\mathbf{B}\|z$. Taking into account the random orientations of the confining structures with respect to $\mathbf{B}$, one finds a mean shift in the resonance line of $\frac{2}{3}\delta g$, and a broadening corresponding to a standard deviation of $0.3\delta g$. At the X-band (~ 9 GHz) frequencies employed in Refs. 40–47, this broadening effect is much smaller than either the experimental broadening or the calculated broadening due to fine-structure splitting (Sec. V), and can be neglected. The small correction to the average g factor is not significant, as comparable corrections may arise from term (3) in a full treatment of the Luttinger EMT Hamiltonian.[25]

(3) H^{ze} can also couple the P_x and P_y states back to the P_z ground state, through the terms that involve $\mathbf{A}$ and $\mathbf{p}_h$ together with the Luttinger parameters γ_2 or γ_3;[25] but these matrix elements vanish unless the envelope function for the lowest P_z state differs from those for the lowest P_x and P_y states. The envelope functions are identical in the simplest approximation to EMT, so that g_{ij} is unchanged.

We conclude that, within the simple theory of the present work, the spin-orbit interaction causes only a small correction to g_{ij}. This can be neglected compared to the large fine-structure splitting discussed in the main text. An exact treatment of the effective-mass theory would calculate the basis states using the full Luttinger Hamiltonian (but not including $H^{\mathrm{SO}}+H^z$). This would require the use of a three-component wave function as in Eq. (10), and would lead to mixing of the pure P_x, P_y, and P_z states employed above, and to differences between the envelope functions that correspond to the dominant P_i components of these states. Corrections to the g factor would then arise from term (3) as well as from term (2). Such a calculation is beyond the scope of the present work.

---

[1] L. T. Canham, Appl. Phys. Lett. **57**, 1046 (1990).

[2] A. G. Cullis and L. T. Canham, Nature **353**, 335 (1991).

[3] P. D. J. Calcott, K. J. Nash, L. T. Canham, M. J. Kane, and D. Brumhead, J. Phys. Condens. Matter **5**, L91 (1993).

[4] P. D. J. Calcott, K. J. Nash, L. T. Canham, M. J. Kane, and D. Brumhead, in *Microcrystalline Semiconductors: Materials Science & Devices,* edited by P. M. Fauchet, C. C. Tsai, L. T. Canham, I. Shimizu, and Y. Aoyagi, MRS Symposia Proceedings No. 283 (Materials Research Society, Pittsburgh, 1993), p. 143.

[5] P. D. J. Calcott, K. J. Nash, L. T. Canham, M. J. Kane, and D. Brumhead, J. Lumin. **57**, 257 (1993).

[6] K. J. Nash, P. D. J. Calcott, L. T. Canham, M. J. Kane, and D. Brumhead, J. Lumin. **60&61**, 297 (1994).

[7] T. Suemoto, K. Tanaka, A. Nakajima, and T. Itakura, Phys. Rev. Lett. **70**, 3659 (1993).

[8] J. A. Kash *et al.* (unpublished).

[9] G. W. 't Hooft, Y. A. R. R. Kessener, G. L. J. A. Rikken, and A. H. J. Venhuizen, Appl. Phys. Lett. **61**, 2344 (1992).

[10] J. C. Vial, A. Bsiesy, G. Fishman, F. Gaspard, R. Herino, M. Ligeon, F. Muller, R. Romestain, and R. M. Macfarlane, in *Microcrystalline Semiconductors: Materials Science & Devices* (Ref. 4), p. 241.

[11] T. Suemoto, K. Tanaka, and A. Nakajima, Phys. Rev. B **49**, 11 005 (1994).

[12] G. Mauckner, T. Walter, T. Baier, K. Thonke, R. Sauer, R. Houbertz, U. Memmert, and R. J. Behm, J. Lumin. **57**, 211 (1993).

[13] A. J. Read, R. J. Needs, K. J. Nash, L. T. Canham, P. D. J. Calcott, and A. Qteish, Phys. Rev. Lett. **69**, 1232 (1992); **70**, 2050(E) (1993).

[14] F. Buda, J. Kohanoff, and M. Parrinello, Phys. Rev. Lett. **69**, 1272 (1992).

[15] T. Ohno, K. Shiraishi, and T. Ogawa, Phys. Rev. Lett. **69**, 2400 (1992).

[16] G. D. Sanders and Y. C. Chang, Phys. Rev. B **45**, 9202 (1992).

[17] M. S. Hybertsen and M. Needels, Phys. Rev. B **48**, 4608 (1993).

[18] C. Delerue, G. Allan, and M. Lannoo, Phys. Rev. B **48**, 11 024 (1993).

[19] C.-Y. Yeh, S. B. Zhang, and A. Zunger, Appl. Phys. Lett. **63**, 3455 (1993).

[20] M. S. Hybertsen, Phys. Rev. Lett. **72**, 1514 (1994).

[21] R. J. Needs, A. J. Read, K. J. Nash, S. Bhattacharjee, A. Qteish, L. T. Canham, and P. D. J. Calcott, Physica A **207**, 411 (1994).

[22] R. J. Needs, S. Bhattacharjee, K. J. Nash, A. Qteish, A. J. Read, and L. T. Canham, Phys. Rev. B **50**, 14 223 (1994).

[23] T. Nishino, M. Takeda, and Y. Hamakawa, Solid State Commun. **14**, 627 (1974).

[24] J. M. Luttinger and W. Kohn, Phys. Rev. **97**, 869 (1955).

[25] J. M. Luttinger, Phys. Rev. **102**, 1030 (1956).

[26] G. D. Watkins and F. S. Ham, Phys. Rev. B **1**, 4071 (1970).

[27] For substitutional donors in silicon, larger spin-valley splittings occur (up to 1 meV for Bi), arising from the spin-orbit interaction of the impurity atom. The spin-valley interaction in Si nanostructures should be compared with that for the interstitial Li donor, which is derived from the spin-orbit interaction of the Si host crystal (Ref. 26).

[28] P. M. Mathews and K. Venkatesan, *A Textbook of Quantum Mechanics* (Tata McGraw-Hill, New Delhi, 1967), p. 285.

[29] T. van Buuren, T. Tiedje, J. R. Dahn, and B. M. Way, Appl. Phys. Lett. **63**, 2911 (1993).

[30] Values of $\gamma_1=4.285$, $\gamma_2=0.339$, $\gamma_3=1.446$, and $\kappa=-0.42$ were obtained by J. C. Hensel [(unpublished) cited in Ref. 31].

[31] *Semiconductors. Physics of Group IV Elements and III-V*

Compounds, edited by O. Madelung *et al.*, Landolt-Börnstein, New Series, Group III, Vol. 17, Pt. a (Springer-Verlag, Berlin, 1982).

[32] B. C. Cavenett, Adv. Phys. **30**, 475 (1981).

[33] K. M. Lee, L. C. Kimerling, B. G. Bagley, and W. E. Quinn, Solid State Commun. **57**, 615 (1986).

[34] A. M. Stoneham, *Theory of Defects in Solids* (Clarendon, Oxford, 1975), Chap. 13 and Appendix II.

[35] J. S. Griffith, *The Theory of Transition Metal Ions* (Cambridge University Press, Cambridge, England, 1961).

[36] A. Abragam and B. Bleaney, *Electron Paramagnetic Resonance of Transition Ions* (Clarendon, Oxford, 1970).

[37] See, for example, K. M. Lee, in *Defects in Electron Materials,* edited by M. Stavola, S. J. Pearton, and G. Davies, MRS Symposia Proceedings No. 104 (Materials Research Society, Pittsburgh, 1988), p. 449; M. Godlewski and B. Monemar, Phys. Rev. B **37**, 2752 (1988).

[38] Reference 43, p. 935, with similar statements in Refs. 42, 44, 45, and 47.

[39] P. A. Lane, L. S. Swanson, J. Shinar, and S. Chumbly, in *Light Emission from Silicon,* edited by S. S. Iyer, R. T. Collins, and L. T. Canham, MRS Symposia Proceeding No. 256 (Materials Research Society, Pittsburgh, 1992), p. 169.

[40] M. S. Brandt and M. Stutzmann, Appl. Phys. Lett. **61**, 2569 (1992).

[41] M. Stutzmann, J. Weber, M. S. Brandt, H. D. Fuchs, M. Rosenbauer, P. Deak, A. Höpner, and A. Breitschwerdt, Festkörperprobleme **32**, 179 (1992).

[42] H. D. Fuchs, M. Rosenbauer, M. S. Brandt, S. Ernst, S. Finkbeiner, M. Stutzmann, K. Syassen, J. Weber, H. J. Queisser, and M. Cardona, in *Microcrystalline Semiconductors: Materials Science & Devices* (Ref. 4), p. 203.

[43] M. Stutzmann, M. S. Brandt, E. Bustarret, H. D. Fuchs, M. Rosenbauer, A. Höpner, and J. Weber, J. Non-Cryst. Solids **164-166**, 931 (1993).

[44] M. Rosenbauer, M. S. Brandt, H. D. Fuchs, A. Höpner, A. Breitschwerdt, and M. Stutzmann, in *Optical Properties of Low Dimensional Silicon Structures,* Vol. 244 of *NATO Advanced Study Institute, Series E: Applied Sciences,* edited by D. C. Bensahel, L. T. Canham, and S. Ossicini (Kluwer, Dordrecht, 1993), p. 43.

[45] M. S. Brandt, M. Rosenbauer, and M. Stutzmann, in *Silicon Based Optoelectronic Materials,* edited by M. A. Tischler, R. T. Collins, M. L. Thewalt, and G. Abstreiter, MRS Symposia Proceedings No. 298 (Materials Research Society, Pittsburgh, 1993), p. 301.

[46] M. Stutzmann, M. S. Brandt, M. Rosenbauer, H. D. Fuchs, S. Finkbeiner, J. Weber, and P. Deak, J. Lumin. **57**, 321 (1993).

[47] M. S. Brandt and M. Stutzmann, Solid State Commun. **93**, 473 (1995).

[48] B. K. Meyer, D. M. Hofmann, W. Stadler, V. Petrova-Koch, F. Koch, P. Omling, and P. Emanuelsson, Appl. Phys. Lett. **63**, 2120 (1993).

[49] B. K. Meyer, D. M. Hofmann, W. Stadler, V. Petrova-Koch, F. Koch, P. Emanuelsson, and P. Omling, J. Lumin. **57**, 137 (1993).

[50] A. Kux and D. M. Hofmann, in *Optical Properties of Low Dimensional Silicon Structures* (Ref. 44), p. 197.

[51] Y. Mochizuki and M. Mizuta, Jpn. J. Appl. Phys. **32**, L1387 (1993).

[52] See, for example, R. A. Street, *Hydrogenated Amorphous Silicon* (Cambridge University Press, Cambridge, England, 1991), p. 106.

[53] Similarly, the spin-orbit interaction causes a small correction to the single-particle energy levels, which can be estimated using perturbation theory, and for most purposes can be neglected (Ref. 22).

[54] Y. Abe, J. Phys. Soc. Jpn. **19**, 818 (1964).

[55] C. H. Henry, R. A. Faulkner, and K. Nassau, Phys. Rev. **183**, 798 (1969).

[56] K. Suzuki and J. C. Hensel, Phys. Rev. B **9**, 4184 (1974).